pH-Induced Reversible Complexation of Poly(ethylene glycol) and Poly(ϵ-caprolactone)-*b*-poly(methacrylic acid) Copolymer Micelles

Sang Cheon Lee,* Kyung Ja Kim, Young-Keun Jeong, Jeong Ho Chang, and Jinsub Choi

Nanomaterials Application Division, Korea Institute of Ceramic Engineering and Technology, Seoul 153-801, Korea

Received June 27, 2005; Revised Manuscript Received August 1, 2005

ABSTRACT: The pH-induced reversible complexation between poly(ethylene glycol) (PEG) and the polymer micelles of a pyrene-labeled poly(ϵ-caprolactone)-*b*-poly(methacrylic acid) copolymer (Py-PCL-*b*-PMAA) was investigated in an aqueous phase. At pH 7.4−4.0, the polymer micelles and PEG existed separately. The complexation began at pH 3.9 through hydrogen-bonding to produce the colloidal hybrid featuring PEG-mediated long-range interconnected micelles. Further pH decrease resulted in the precipitation of the white complex hybrid in water. This pH-dependent complexation was a reversible process. The polymer micelles in the solid complex hybrid could be quantified by fluorescence spectroscopy. The pyrene fluorescence intensity of the aqueous mixture was constant in the pH range 7.4−4.0, indicating that the solid hybrids were not formed, whereas the pH decrease to 3.9 resulted in the decrease of fluorescence intensity at a level of 58.5%, indicating complexation of 58.5% micelles into the solid hybrid. The pyrene fluorescence intensity at pH below 3.5 corresponded to about 0.1% of that of the initial micelle solution prepared at pH 7.4, reflecting that about 100% of the micelles are complexed with PEG to form the solid hybrid. The micelles assembled in the hybrid could be reversibly dispersed as micelles at pH > 4.0. The pH-controlled release experiments showed that the micelles could be redispersed from the hybrid at physiological pH (pH 7.4), whereas at an acidic pH (pH 2.0) the micelle release was completely prohibited.

Introduction

A diverse class of self-assembled systems such as polymer/polymer,[1,2] polymer/nanoparticle,[3−7] and nanoparticle/nanoparticle[8] has attracted expanding interest due to its usefulness in generation of novel assembly systems with tunable properties for various applications such as biotechnology and microelectronics. In particular, polymer/nanoparticle hybrids constructed by polymer-mediated assembly of nanoparticles are functional materials with versatile utilities.[9,10] The use of polymers and nanoparticles designed for specific interspecies interaction such as hydrogen-bonding and oppositely charged ionic interactions have created nanohybrids featuring programmed structures and properties.[9] Rotello et al. have reported extensively on the structural control and applications of many kinds of polymer/nanoparticle assembly systems.[3−5,9,10] As representative examples, using gold or iron oxide nanoparticles, they showed that polymers functionalized with recognition elements could be used for ordering of nanoparticles into structured assemblies by the "bricks and mortar" approach through a hydrogen-bonding interaction.[3,4] To date, various polymer systems including dendrimers and homopolymers or block copolymers with specific ligands capable of interacting with nanoparticles have been employed to extend the scope of this methodology.[3,5,11] For nanoparticles, surface-functionalized metal and semiconductor nanoparticles such as gold, iron oxide, and palladium were main components.[4,12,13]

* Author to whom correspondence should be addressed: Sang Cheon Lee, Ph.D., Nanomaterials Application Division, Korea Institute of Ceramic Engineering and Technology, 233-5 Gasan-Dong, Guemcheon-Gu, Seoul 153-801, Korea. Tel: 82-2-3282-2469. Fax: 82-2-3282-7769. E-mail: sclee@kicet.re.kr.

Recently, stimuli-controlled reversible assembly between polymers and nanoparticles has been an issue in the growing field of intelligent nanohybrids.[6,14] Combination of polymer/nanoparticle systems with reversible interaction offers an attractive approach of providing nanohybrids responsive to chemical or thermal stimulus.[14,15] Mori et al. reported on the novel intelligent colloidal polymer/silica nanocomposites, where the complexation of cationic silica nanoparticles and a weak anionic polyelectrolyte can be manipulated simply by pH change.[14]

Polymeric micelles assembled from amphiphilic block copolymers have found a wide range of applications including drug delivery, encapsulation, and nano-reactors.[16] The unique characteristics of polymer micelles as nanoparticles lie in nanosize, core−shell structure, and easily controllable surface functionality. Thus, polymer micelles may act as a good building block for constructing new kinds of polymer/nanoparticle assembly. In particular, polymer/micelle nanohybrids of which the assembly/disassembly state can be controlled in response to external stimuli may open the new application field.

In this work, we describe reversible pH-induced complexation of poly(ethylene glycol) (PEG) and the polymer micelles of pyrene-labeled poly(ϵ-caprolactone)-*b*-poly(methacrylic acid) copolymer. In an aqueous phase, a weak anionic polyelectrolyte PMAA constructing micellar shell is known to undergo pH-dependent reversible complexation with PEG through hydrogen-bonding.[17,18] To date, most of studies were focused on complexation between PMAA and PEG homopolymers in a single molecular level. In this study, we aim to extend this complexation approach to nanohybrids consisting of PEG and the polymer micelles with the PMAA outer shell. The reversible pH-induced complex-

10.1021/ma051380h CCC: $30.25
Published on Web 09/30/2005

ation and complex hybrid formation between PEG and the Py-PCL-*b*-PMAA micelles were examined by fluorescence spectroscopy, dynamic light scattering, and transmission electron microscopy (TEM). The reversible release behavior of the polymer micelles from the complex hybrids was also estimated by controlling pH.

Experimental Section

Materials and Equipment. Ethylene glycol (EG), trifluoroacetic acid (TFA), 1-pyrenebutyric acid, 1,3-dicyclohexylcarbodiimide (DCC), 4-(dimethylamino)pyridine (DMAP), *tert*-butyl methacrylate (tBMA), copper(I) bromide (Cu(I)Br, 99.999%), *N*,*N*,*N*′,*N*′,*N*″-pentamethyldiethylenetriamine (PMDETA), poly(ethylene glycol) (M_n: 5000) (PEG), and a 2.0 M HCl solution in diethyl ether (Et_2O) were purchased from Aldrich Co. (Milwaukee, WI) and used without further purification. 2-Bromopropionyl bromide (BPB) was purchased from Aldrich Co. (Milwaukee, WI) and freshly distilled under vacuum. ϵ-Caprolactone (CL), 2-ethyl-2-oxazoline (EtOz), and methyl *p*-toluenesulfonate were purchased from Aldrich Co. (Milwaukee, WI), dried over calcium hydride, and vacuum distilled. Tetrahydrofuran (THF) and toluene were distilled from Na/benzophenone under N_2, prior to use. Triethylamine (TEA), acetonitrile, and methylene chloride were dried and distilled over calcium hydride. Diethyl ether and *n*-hexane were of the reagent grade. ^{1}H spectra were obtained on a FT-NMR spectrometer (Varian, Unity plus, CA) at 300 MHz. Elemental analysis was performed on a PerkinElmer Series II CHNS/O Analyzer 2400. Molecular weights and molecular weight distributions were determined using a GPC equipped with a Waters 2414 refractive index detector, 515 HPLC pump, and three consecutive Styragel columns (HR1, HR2, and HR4). The eluent was THF with a flow rate of 1 mL/min. The molecular weights were calibrated with polystyrene standards.

2-Hydroxyethyl 2′-Bromopropionate (HEBP). A solution of EG (43 g, 0.69 mol) and TEA (8.4 g, 0.08 mol) in dry methylene chloride (250 mL) was placed into the flame-dried two-neck round-bottom flask equipped with a condenser, a dropping funnel, N_2 inlet/outlet, and a magnetic stirrer. After cooling to 0 °C, BPB (15 g, 0.069 mol) in dry methylene chloride (50 mL) was then added dropwise to the stirred solution. The reaction mixture was stirred at room temperature under nitrogen for 24 h. The reaction mixture was filtered to remove precipitates, and the solvent was evaporated under pressure. The mixture was dissolved in distilled water (100 mL) and extracted with chloroform (3 × 300 mL). The organic phase was dried over anhydrous magnesium sulfate and filtered. After solvent evaporation, pure HEBP was isolated by vacuum distillation (bp 70 °C at 1.0 mmHg). Yield 60%. ^{1}H NMR (DMSO-d_6): δ 1.71 (d, J = 7.0 Hz, 3H, CH(C***H***$_3$)Br), 3.57 (t, J = 5.0 Hz, 2H, HOC***H***$_2$CH$_2$O−), 4.08 (t, J = 5.0 Hz, 2H, HOCH$_2$C***H***$_2$O−), 4.64 (q, J = 7.0 Hz, 1H, C***H***(CH$_3$)Br), 5.0 (s, 1H, ***H***OCH$_2$CH$_2$O−). Anal. Calcd for $C_5H_9O_3Br$: C, 30.48; H, 4.60. Found: C, 30.60; H, 4.96.

α-Bromopropionyl-ω-hydroxy PCL (HO-PCL-Br). To a stirred solution of ϵ-caprolactone (15 g, 0.13 mol) in methylene chloride (70 mL) was added HEBP (0.86 g, 0.0044 mol). The polymerization was initiated by the addition of 4.35 mL (0.0087 mol) of HCl solution (2 M) in diethyl ether at 25 °C, and the reaction mixture was stirred under N_2 for 24 h. The HO-PCL-Br was isolated by precipitation from methylene chloride into *n*-hexane (700 mL). Yield 99%. ^{1}H NMR ($CDCl_3$): 1.28 (m, CO(CH$_2$)$_2$C***H***$_2$(CH$_2$)$_2$O), 1.52 (m, COCH$_2$C***H***$_2$CH$_2$C***H***$_2$CH$_2$O), 1.71 (d, J = 7.0 Hz, COCHC***H***$_3$Br), 2.26 (t, J = 7.5 Hz, COC***H***$_2$-(CH$_2$)$_4$O), 3.97 (t, J = 6.6 Hz, CO(CH$_2$)$_4$C***H***$_2$O), 4.63 (q, J = 7.0 Hz, COC***H***CH$_3$Br).

HO-PCL-*b*-poly(*tert*-butyl methacrylate) (HO-PCL-*b*-PtBMA). The HO-PCL-Br macroinitiator (3 g, 0.86 mmol) and Cu(I)Br (0.49 g, 3.4 mmol) were added to a flame-dried round-bottom flask. The flask was evacuated and refilled with dry nitrogen twice. Toluene (10 mL), *t*BMA (4.88 g, 34 mmol), and PMDETA (0.054 g, 0.32 mmol) were degassed separately by N_2 and introduced into the reaction flask. The flask was placed in a preheated oil bath at 85 °C. The reaction was maintained for 15 h under N_2. The reaction solution became gradually viscous. After the polymerization, the reaction mixture was diluted with THF and passed through neutral alumina to remove the copper catalyst. The block copolymers were purified by precipitation from THF into cold *n*-hexane. Yield 70%. ^{1}H NMR ($CDCl_3$): δ 1.11−1.91 (br m, C***H***$_2$(C***H***$_3$)CHCOOC(CH$_3$)$_3$), 1.28 (m, CO(CH$_2$)$_2$C***H***$_2$(CH$_2$)$_2$O), 1.44 (s, CH$_2$(CH$_3$)CHCOOC-(C***H***$_3$)$_3$), 1.52 (m, COCH$_2$C***H***$_2$CH$_2$C***H***$_2$CH$_2$O), 2.11−2.31 (br, CH$_2$(CH$_3$)C***H***COOC(CH$_3$)$_3$), 2.26 (t, J = 7.5 Hz, COC***H***$_2$-(CH$_2$)$_4$O), 3.97 (t, J = 6.6 Hz, CO(CH$_2$)$_4$C***H***$_2$O).

Pyrene-Labeled PCL-*b*-PtBMA (Py-PCL-*b*-PtBMA). Pyrene was labeled at the terminal of the PCL block by DCC chemistry. To a stirred solution of HO-PCL-*b*-PtBMA (3.5 g, 0.4 mmol) and 1-pyrenebutyric acid (0.13, 0.4 mmol) in dry THF (15 mL) was added a solution of DCC (0.19 g, 0.9 mmol) and DMAP (0.02 g, 0.2 mmol) in dry THF (1 mL). The reaction mixture was stirred at room temperature for 24 h. Py-PCL-*b*-PtBMA was isolated by repeated precipitation from THF into *n*-hexane. Yield 98%. ^{1}H NMR ($CDCl_3$): δ 1.1.−1.9 (br m, C***H***$_2$-(C***H***$_3$)CHCOOC(CH$_3$)$_3$), 1.28 (m, CO(CH$_2$)$_2$C***H***$_2$(CH$_2$)$_2$O), 1.44 (s, CH$_2$(CH$_3$)CHCOOC(C***H***$_3$)$_3$), 1.52 (m, COCH$_2$C***H***$_2$CH$_2$C***H***$_2$-CH$_2$O), 2.1−2.3 (br, CH$_2$(CH$_3$)C***H***COOC(CH$_3$)$_3$), 2.26 (t, J = 7.5 Hz, COC***H***$_2$(CH$_2$)$_4$O), 3.97 (t, J = 6.6 Hz, CO(CH$_2$)$_4$C***H***$_2$O), 7.9−8.3 (m, pyrenyl protons).

Hydrolysis of Py-PCL-*b*-PtBMA for Py-PCL-*b*-PMAA. To a solution of Py-PCL-*b*-PtBMA (2.5 g, 0.3 mmol) in methylene chloride, trifluoroacetic acid (TFA) (10 mL, 0.13 mol) was slowly added at 0 °C with vigorous stirring. The reaction mixture was stirred at 0 °C for 3 h and at 25 °C for 3 h. To obtain a final product (Py-PCL-*b*-PMAA), the crude product was dissolved in distilled water, and the solution was then dialyzed using a membrane (MWCO: 1000) for 24 h, followed by freeze-drying. Yield 95%. ^{1}H NMR (THF-d_8/D_2O = 10/1): δ 1.26 (m, CO(CH$_2$)$_2$C***H***$_2$(CH$_2$)$_2$O), 1.48−2.12 (C***H***$_2$-(C***H***$_3$)COOH), 1.59 (m, COCH$_2$C***H***$_2$CH$_2$C***H***$_2$CH$_2$O), 2.21−2.52 (br, CH$_2$(CH$_3$)C***H***COOH), 2.29 (t, J = 7.5 Hz, COC***H***$_2$(CH$_2$)$_4$O), 3.97 (t, J = 6.6 Hz, CO(CH$_2$)$_4$C***H***$_2$O), 8.12−8.61 (m, pyrenyl protons). ^{1}H NMR analysis showed that *tert*-butyl groups disappeared completely after the hydrolysis using TFA.

Poly(2-ethyl-2-oxazoline) (PEtOz) (M_n: 11000 g/mol). A solution of 2-ethyl-2-oxazoline (10.00 g, 0.1 mmol) and methyl *p*-toluenesulfonate (0.17 g, 0.9 mmol) in acetonitrile (300 mL) was stirred at reflux for 30 h under nitrogen. The product, PEtOz, was isolated following a reference procedure.[19] Yield 95%. ^{1}H NMR ($CDCl_3$): δ 1.21 (br, (CO)NCH$_2$C***H***$_3$), 2.31 (br, (CO)NC***H***$_2$CH$_3$), 3,41 (br, C***H***$_2$N(CO)C***H***$_2$).

Fluorescence Measurements. Pyrene fluorescence spectra were recorded on a JASCO FP-6500 spectrofluorometer. The concentration of sample solutions was varied from 1 × 10^{-4} to 5 g/L. For the measurement of pyrene emission spectra, emission and excitation bandwidths were set at 5 nm. The excitation wavelength was 336 nm, and λ_{em} = 395 nm. The spectra were accumulated with an integration of 3 s/nm.

Light-Scattering Measurements. Dynamic light-scattering measurements were performed using a 90 Plus particle size analyzer (Brookhaven Instruments Corporation). All the measurements were carried out at 25 °C. The sample solutions were purified by passing through a Millipore 0.45-μm filter. The scattered light of a vertically polarized He−Ne laser (632.8 nm) was measured at an angle of 90° and was collected on an autocorrelator. The hydrodynamic diameters (d) of micelles were calculated by using the Stokes−Einstein equation $d = k_BT/3\pi\eta D$ where k_B is the Boltzmann constant, T is the absolute temperature, η is the solvent viscosity, and D is the diffusion coefficient. The polydispersity factor of micelles, represented as μ_2/Γ^2, where μ_2 is the second cumulant of the decay function and Γ is the average characteristic line width, was calculated from the cumulant method.[20] CONTIN algorithms were used in the Laplace inversion of the autocorrelation function to obtain micelle size distribution.[21]

Transmission Electron Microscopy. Transmission electron microscopy (TEM) was performed on a Philips CM 200, operating at an acceleration voltage of 80 kV. For the observation of size and distribution of micellar particles, a drop of

Scheme 1. Synthetic Route for Py-PCL-*b*-PMAA

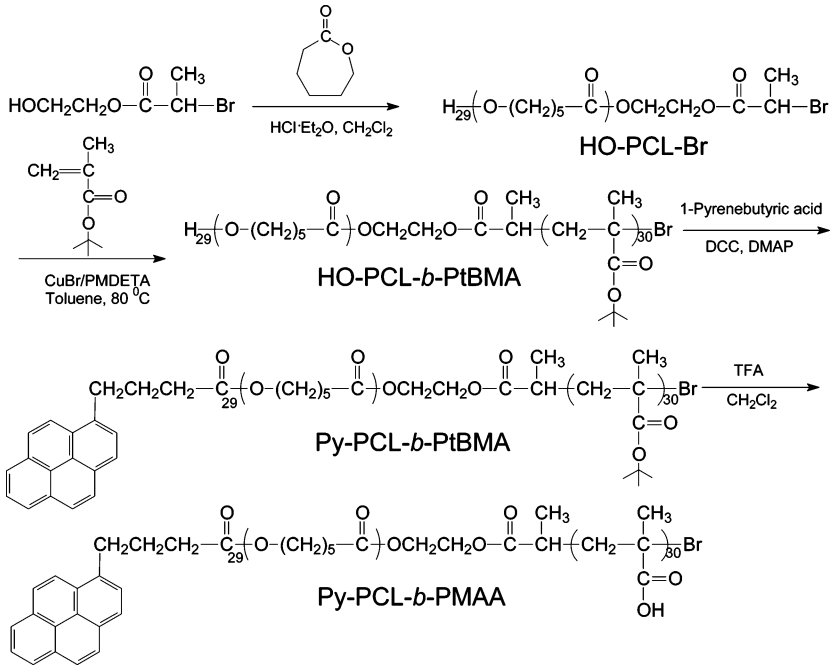

sample solution (concentration = 1 g/L) was placed onto a 200-mesh copper grid coated with carbon. About 2 min after deposition, the grid was tapped with a filter paper to remove surface water, followed by air-drying. Negative staining was performed by using a droplet of a 5 wt % uranyl acetate solution. The samples were air-dried before measurement.[22]

pH-Dependent Complexation of Py-PCL-*b*-PMAA Micelles with PEG. The Py-PCL-*b*-PMAA micellar solutions (10 mL, concentration = 1 g/L) were mixed with PEG at pH 7.4. The pH of the mixture of the micellar solutions and PEG was then adjusted in the range of 2.0−7.4 (pH 2.0, 3.0, 3.5, 3.7, 3.9, 4.0, 4.5, 5.0, 6.0, 7.4). The hybrid formation of the micelles with PEG at prefixed pH was examined by monitoring the change in pyrene fluorescence intensity of the aqueous mixture, and the structure of the hybrids in the solution was visualized by TEM. For quantification of the micelles in the complex solid hybrid, the mixture at each pH was centrifuged at 3000 rpm for 30 min, and the supernatant was analyzed by fluorescence spectroscopy. The quantity of micelles in the solid hybrid was calculated by the ratio of pyrene fluorescence intensity (I) of the micelle/PEG mixture at each pH to the initial fluorescence intensity (I_0) of Py-PCL-*b*-PMAA micelle solutions prepared initially at pH 7.4. The mixture of Py-PCL-*b*-PMAA micelles and water-soluble PEtOz was also examined to compare its complexation behavior with that of the Py-PCL-*b*-PMAA micelles/PEG system.

Reversible pH-Controlled Micelle Release from the Complex Hybrids. For the reversible release of micelles from the complex, the precipitated micelle/PEG hybrids were recovered, freeze-dried, and pressed as a disk with a diameter of 100 mm and a thickness of 0.5 mm. The release behavior of the micelles from the complex was investigated in phosphate buffer solutions (pH 7.4, 5.5, and pH 2.0). The concentrations of all the media were 100 mM with identical ionic strength. The disc-shaped hybrid was placed in a screw-capped tube containing 10 mL of release medium. The tube was placed in a shaker bath maintained at 37 °C and shaken horizontally at 200 rpm. At predetermined time intervals, 5 mL of solutions were withdrawn from the release medium and replaced with an equal volume of fresh medium. The samples were assayed using a spectrofluorometer. In our assumption, the number of micelles is in a linear relationship with the concentration of block copolymer solutions above the critical micelle concentration (cmc), and the pyrene fluorescence intensity also has an identical relationship with the number of micelles in the solutions. The micelle release was quantified by the pyrene fluorescence. For quantitative analysis for the micelles release, the standard curves for polymer concentrations could be obtained by the calibration of pyrene fluorescence intensities in the micelle solutions of various block copolymer concentrations (0.001−0.05 g/L). The concentration of block copolymer solution (g/L) = (intensity at 395 nm − 0.13)/3046, $r^2 = 0.9999$. The pH-dependent release behavior of the pyrene-loaded micelle from the hybrid was investigated by varying the pH of the release medium.

Results and Discussion

Synthesis of Py-PCL-*b*-PMAA. An amphiphilic block copolymer of PCL and PMAA was synthesized following a multistep synthetic procedure illustrated in Scheme 1. Basically, the copolymer synthesis was based on a two-step controlled pseudo-living polymerization. Pyrene moieties were labeled at the terminal of the PCL block to provide polymer micelles with a photophysical property useful for assembly/disassembly assay in an aqueous phase. First, using a modified literature procedure,[23] a macroinitiator (HO-PCL-Br) was synthesized by activated cationic polymerization of ϵ-caprolactone using 2-hydroxyethyl 2′-bromopropionate prepared by the reaction of ethylene glycol with 2-bromopropionyl bromide.

The number average molecular weight (M_n) of HO-PCL-Br was calculated by the peak integration ratio of C***H*** in the 2-bromopropionate end group at 4.63 ppm to C***H***$_2$ protons in the PCL repeating unit at 3.97 ppm. The M_n of HO-PCL-Br was estimated to be 3500 g/mol. GPC analysis showed that the HO-PCL-Br macroinitiator had a narrow molecular weight distribution (M_w/M_n = 1.15). In the second step, the HO-PCL-Br macroinitiator was used to produce block copolymers, HO-PCL-*b*-PtBMA, by atom transfer radical polymerization (ATRP) of *tert*-butyl methacrylate (tBMA). ATRP was carried out by heating a mixture of HO-PCL-Br and tBMA in the presence of an excess, relative to initiating species, of equal amounts of Cu(I)Br and PMDETA at 80 °C. The molecular weight, molecular weight distribution, and the block composition of the copolymer were determined by ^{1}H NMR and GPC. As listed in Table 1, conversion

Table 1. Characteristics of Py-PCL-*b*-PMAA

copolymer[a]	feed ratio ([CL]:[tBMA])	composition ratio ([CL]:[MAA])[b]	conversion (%)[b]	M_n[b]	M_w/M_n[c]
Py-PCL-*b*-PMAA	29:43	29:30	70	7860	1.21

[a] The copolymer was synthesized using the macroinitiator (HO-PCL-Br) with a M_n of 3500 and polydispersity of 1.15, respectively. [b] Calculated by ^{1}H NMR spectra. [c] Estimated by GPC.

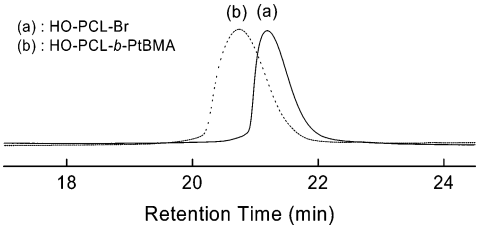

Figure 1. Gel permeation chromatograms of HO-PCL-Br (a) and HO-PCL-*b*-PtBMA (b).

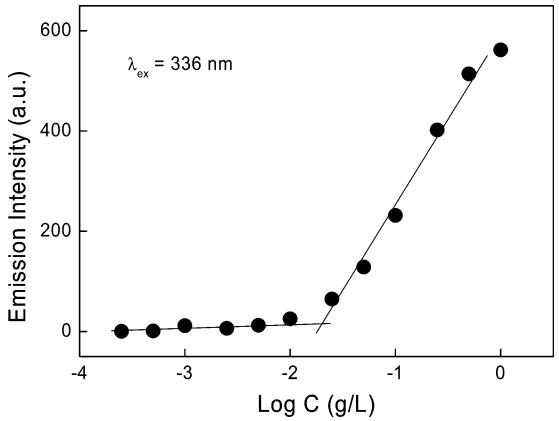

Figure 2. Plot of pyrene emission intensity vs log *C* of the Py-PCL-*b*-PMAA copolymer.

for polymerization of tBMA was 70%, and the composition ratio of repeating units in PCL and PtBMA was estimated to be 29:30.

Figure 1 shows GPC chromatograms of the macroinitiator (HO-PCL-Br) and the resultant diblock copolymer, HO-PCL-*b*-PtBMA. The block copolymer exhibited a narrow GPC trace with polydispersity of 1.21 (Table 1). This indicates that HO-PCL-Br was involved efficiently in initiating ATRP of tBMA, and there were no uncontrolled side reactions, particularly thermal polymerization. Pyrene labeling was successfully performed by a DCC-mediated coupling reaction between the hydroxyl end group of the PCL block and the carboxyl group of pyrenebutyric acid. The final product, Py-PCL-*b*-PMAA, was obtained from the selective hydrolysis of the *tert*-butyl ester groups in Py-PCL-*b*-PtBMA using TFA. As described in the Experimental Section, the resonance for the *tert*-butyl ester groups of PtBMA completely disappeared after the reaction with TFA. The amphiphilic character of Py-PCL-*b*-PMAA gives an opportunity to self-associate in water to form a core−shell-type micelle structure. Thus, the polymer design in this work is useful for production of the polymer micelles with a functionalized nanosurface with carboxylic groups of which the protonation/ionization state can be controlled by pH.

Micelles of Py-PCL-*b*-PMAA. The micelle formation of the block copolymer in an aqueous phase was confirmed by a fluorescence technique using pyrene as a probe.[24,25] The amphiphilic Py-PCL-*b*-PMAA copolymer is expected to self-associate in water to form polymer micelles of the hydrophobic PCL inner core and

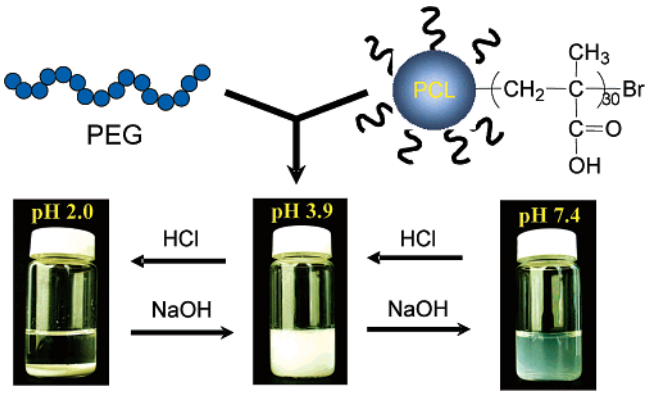

Figure 3. pH-dependent phase behavior of the mixture of PEG and Py-PCL-*b*-PMAA micelles.

the hydrated PMAA outer shell. Upon micellization in water, pyrene moieties labeled at the PCL terminal preferably locate inside or close to the hydrophobic microdomain of micelles, and consequently their quantum yield increases due to the lowered environmental polarity, compared with the water environment.[26] The characteristic increase of the pyrene emission intensity, upon pyrene partition into the micellar hydrophobic microdomain, was utilized to determine the cmc value of Py-PCL-*b*-PMAA. Figure 2 shows the intensity change of pyrene emission versus the logarithm of the Py-PCL-*b*-PMAA copolymer concentration. The critical micelle concentration was determined from the threshold concentration, where emission intensity began to show substantial increase. Therefore, the interception of two straight lines is determined as cmc. The cmc value of the Py-PCL-*b*-PMAA copolymer was determined to be 20 mg/L. The hydrodynamic diameters of the micelles from dynamic light scattering were 70 nm, with a narrow polydispersity factor of 0.09 (μ_2/Γ^2). The pH-dependent stability of the Py-PCL-*b*-PMAA micelles was examined by measuring the hydrodynamic diameter at various pH ranges. The micelle size was 70 nm above pH 4.0, whereas a pH decrease below 4.0 resulted in the size decrease to 48 nm, probably due to the hydrogen-bonding within the protonated PMAA outer shell. This indicates that the structure of the hydrated corona of the micelles became more compact with decreasing pH. But, the narrow size distribution was maintained at a pH below 4.0 ($(\mu_2/\Gamma^2 = 0.1)$. This strongly supports the concept that the micelles were stable without aggregation, even at low pH. The micelles of Py-PCL-*b*-PMAA were visualized by TEM, as shown in Figure 4a. The micelles of the Py-PCL-*b*-PMAA copolymer were generally spherical. The micelle sizes visualized by TEM were a little smaller than those measured by dynamic light scattering, probably due to the drying process for TEM measurements.

pH-Controlled Complexation of the Py-PCL-*b*-PMAA Micelles and PEG. pH-dependent assembly based on complexation between Py-PCL-*b*-PMAA micelles and PEG was investigated in an aqueous phase. Figure 3 shows the pH-dependent phase behavior of the mixture of Py-PCL-*b*-PMAA micelles and PEG. At pH

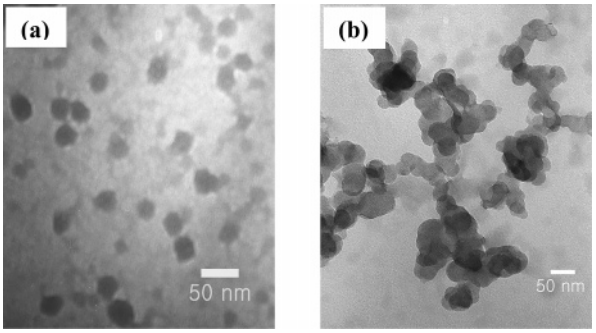

Figure 4. TEM images of the individual micelles from the micelles/PEG mixture at pH 7.4 (a) and PEG/micelles hybrid obtained from turbid colloidal dispersion at pH 3.9 (b).

7.4, the polymer micelles and PEG existed separately since most carboxyl groups of PMAA are ionized, and thus hydrogen-bonding interaction between PEG and PMAA is negligible. The complexation began at pH 3.9 to produce colloidal hybrids of hydrogen-bonding-induced long-range interconnected micelles, thereby leading to a white milky dispersion with enhanced light scattering. This complexation is caused by the PEG-mediated intermicellar assembly at specific pH, where the hydrogen-bonding between hydrogen atoms in protonated carboxyl groups and proton-accepting oxygen atoms in PEG repeating units becomes markedly pronounced. The interconnected micelles formed at pH 3.9 behave as a microscale micellar assembly. The structure was neither the gel-like network nor the discrete micelle. The solution had a fair degree of fluidity. It seems that PEG may cross-link the adjacent micelles only in a local region, and, upon hydrogen-bonding-induced assembly of the micelles by PEG, the volume shrinking of the micelles into a specific region is expected. Thus, irrespective of the PEG amount, the PEG/micelle mixture did not form the gel-like structure. Interestingly, upon further decreasing pH to 2.0, the white solid precipitates were formed, probably due to the solubility loss of the PEG/micelle assembly in an aqueous medium.

Figure 4a shows a TEM image of the individual micelles from the micelles/PEG mixture at pH 7.4, and Figure 4b shows a TEM image from the micelles/PEG complex hybrid obtained from turbid dispersion prepared at pH 3.9. These nanoscale images support well the pH-dependent macroscopic phase behavior of the mixtures described in Figure 3. Thus, pH control could lead to the long-range intermicellar assembly by linear PEG, where PEG chains acted as intermicellar bridges. Further pH decrease resulted in the solid precipitation of complex hybrids in water, as shown in Figure 3. This complexation behavior was totally reversible, and the complex hybrids were reversilbly dispersed as individual micelles via pH increase. The mixture of PEG and the polymer micelles at various pH values was centrifuged, and the upper solutions were analyzed by pyrene fluorescence to quantify the complexed micelles in the solid hybrids. Figure 5 shows the pH-dependency of pyrene emission spectra of the mixtures obtained at various pH values.

The variation of pyrene fluorescence intensity at pH range 7.0−4.0 is negligible, but the pH decrease to 3.9 leads to the abrupt decrease of the intensity, reflecting the initiation of the formation of the precipitated micelles/PEG hybrids through hydrogen-bonding. It is of interest to note that the pyrene intensity below pH 3.5 corresponds to about 0.1% of the initial intensity of the

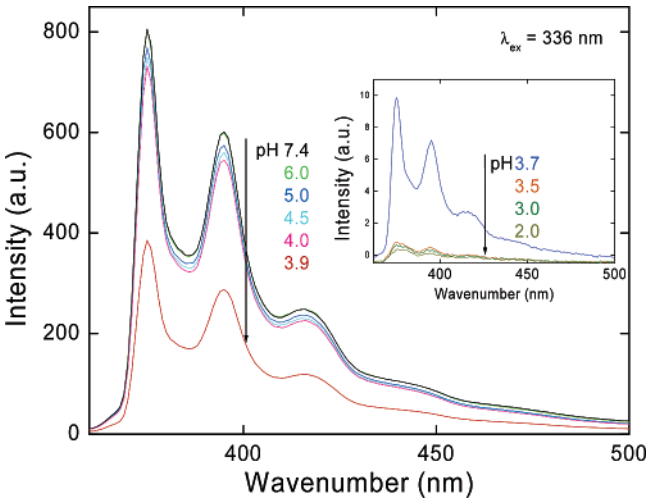

Figure 5. pH-dependent changes in the pyrene fluorescence intensity of the PEG/ micelles mixture.

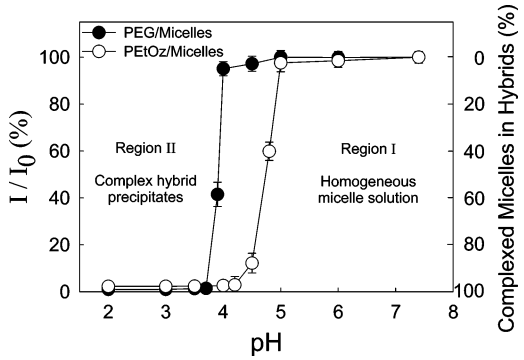

Figure 6. Quantification of the micelles in the solid hybrids. (●): PEG/micelles mixture and (○): PEtOz/micelles mixture.

micelle solution, reflecting participation of almost all the micelles in complex hybrid formation. Figure 6 shows the change of the intensity ratio (I/I_0) of pyrene fluorescence (I) at various pH to initial fluorescence of the micelles (I_0). The $(1 - I/I_0) \times 100$ value represents the percentage of the micelles complexed in the solid hybrids. We note that the complex hybrids are obtained in a 58.5% yield at pH 3.9, and nearly 100% micelles are complexed with PEG at pH below 3.5 to form solid hybrids. This indicates that colloidal polymer micelles can be recovered 100% in the solid state by pH-induced polymer-mediated micelle assembly. A class of water-soluble polymers for this kind of pH-induced micelle complexation can be extended to a variety of proton-accepting polymers. To provide an alternative system and get an idea about the structural effect on complexation behavior, poly(2-ethyl-2-oxazoline) (PEtOz) (−CH_2-CH_2N(O=C−CH_2CH_3)−) with nearly the same repeating unit as with PEG was examined for its ability to induce intermicellar assembly via complexation. PEtOz is known to undergo reversible complexation through hydrogen-bonding with poly(carboxylic acid)s such as PMAA and poly(acrylic acid) (PAA) in an acidic aqueous medium.[27,28] As shown in Figure 6, it is noteworthy that PEtOz induces the intermicellar association to form solid hybrids at a higher pH range than in the case of micelles/PEG mixtures. It is likely that, since PEtOz has two proton-accepting atoms in the repeating units (nitrogen and carbonyl oxygen), the hydrogen-bonding capacity of PEtOz is much stronger than that of PEG, thereby resulting in polymer/micelle complex hybrid formation at higher pH. This indicates that pH-induced

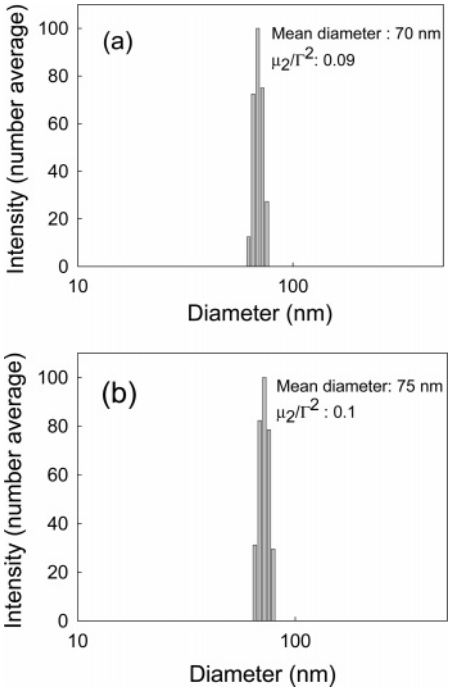

Figure 7. Size distribution of Py-PCL-*b*-PMAA micelles in a phosphate-buffered saline (PBS) solution (pH 7.4) before hybrid formation (a) and after redispersion from the hybrid (b).

polymer/micelles assembly behavior can be controlled depending on the polymer structure. Poly(vinyl alcohol) and poly(vinyl pyrrolidone) are possible alternatives due to their hydrogen-bonding capacity with PMAA. It was noted that the micelle alone could not induce the long-range aggregation of the micelles, and the solid precipitation was not observed by simply lowering the pH of the micelle solution. Only in the case of using polymers such as PEG and PEtOz, the PCL-*b*-PMAA micelles formed the solid precipitates at low pH through the polymer-mediated long-range micellar assembly.

pH-Dependent Reversible Release of the Micelles from the Complex. The complex hybrid of PEG and the micelles were redispersed at pH > 4.0 as a result of disrupting hydrogen-bonding between PEG and the PMAA outer shell of the micelles. The release of micelles from the complex was confirmed by comparing hydrodynamic diameters of the released micelles with those of the micelles before complex formation in PBS solutions. Figure 7, parts a and b, show, respectively, the size distributions of the Py-PCL-*b*-PMAA micelles before hybrid formation and those of redispersed micelles from the hybrid in the PBS (pH 7.4) solution.

As obviously shown in the size distribution, the redispersed solution of the complex hybrid contains the micelles of which hydrodynamic diameters are comparable to those of micelles that are measured before complex formation. This indicates that the micelle structure can be maintained during a pH-controlled assembly/disassembly process. Figure 8 shows the in-vitro release of Py-PCL-*b*-PMAA micelles from the complex hybrid in buffer solutions with pH values of 5.5 and 7.4 at 37 °C.

It was noted that the micelle release from the hybrid was considerably influenced by the pH of the medium, where the more basic the release medium, the higher the rate of the micelle release. In terms of the stability of the hybrid, this result also indicated that the hybrid

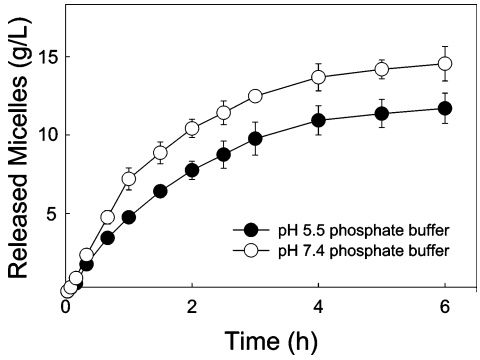

Figure 8. pH-dependent micelle release from the hybrids.

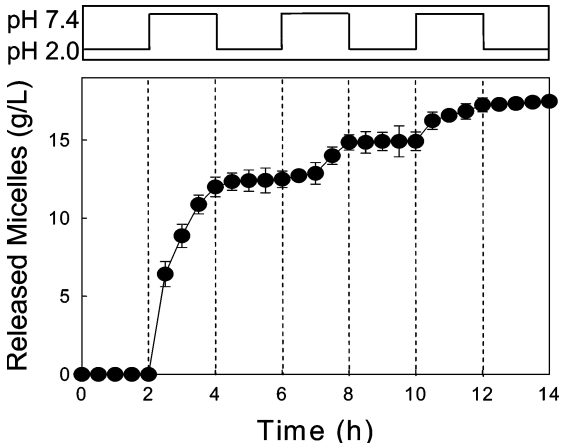

Figure 9. pH-controlled on−off release of the micelles from the hybrid.

in the medium with higher basicity was less stable because the dissolution of the hybrids by the breakage of hydrogen-bonding was highly present. Figure 9 shows on−off micelle release from the hybrid by consecutive pH control.

The micelle release from the hybrid was completely prohibited at pH 2.0, where hydrogen-bonding in the hybrid was maintained. On the other hand, it is noteworthy that the micelle release could be triggered by increasing pH to 7.4. The consecutive pH change can control the storage of micelles or redispersion of micelles from the hybrids.

The polymer components PEG, PCL, and PMAA used for the hybrid formation in this work are widely used as biocompatible materials with low toxicity. In case drug-loaded PCL-*b*-PMAA micelles are used for the complex hybrid, this type of pH-controlled reversible complexation can provide a new platform methodology in the area of oral drug delivery. The main limitation for developing successful oral formulations is the rapid release of drugs unstable at an acidic pH during the transit of the stomach (pH ~ 2.0).[29,30] The hybrid formed by pH-induced complexation of the micelles and polymers can provide a promising matrix that can release the drug-loaded micelles selectively at pH of the small intestine (pH ~ 7.4), thereby maximizing the oral bioavailability of drugs. Besides, the released micelles are expected to adhere to the intestinal wall to deliver drugs efficiently into the blood stream due to the strong mucoadhesive property of the PMAA outer shell.

Conclusions

A new type of pH-controlled reversible complexation between Py-PCL-*b*-PMAA micelles and PEG was inves-

tigated in an aqueous medium. The phase of the PEG/micelle mixture could be conveniently controlled by pH. As pH decreased from 7.4 to 2.0, the mixture of the micelles and PEG underwent a three-stage phase behavior. The Py-PCL-*b*-PMAA micelles and PEG existed separately at pH range of 7.0−4.0. At pH 3.9, PEG induced the long-range interconnection of micelles via hydrogen-bonding with partially protonated PMAA shells. Further pH decrease resulted in the solid precipitation of micelles/PEG complex hybrids. The fluorescence quantification assay showed that nearly 100% micelles in the solution could be recovered in the solid hybrid by pH-induced complexation. This pH-dependent complexation was a reversible process, and the micelles from the complex could be redispersed by increasing pH above 4.0. The micelle release from the complex hybrid could be conveniently controlled by adjusting the pH of release medium.

The concept presented in this study can be extended to a variety of novel intelligent assembly systems. The appropriate selection of many kinds of polymer micelles and the polymer may broaden the scope of nanohybrids of which properties can be tailored to various application fields including controlled delivery and chemical sensing systems.

Acknowledgment. This research was supported by a grant (code no.: 05K1501-01510) from "*Center for Nanostructured Materials Technology*" under "*21st Century Frontier R&D Programs*" of the Ministry of Science and Technology, Korea.

References and Notes

(1) Khutoryanskiy, V. V.; Dubolazov, A. V.; Nurkeeva, Z. S.; Mun, G. A. *Langmuir* **2004**, *20*, 3785−3790.
(2) Mun, G. A.; Nurkeeva, Z. S.; Khutoryanskiy, V. V.; Sergaziyev, A. D. *Colloid Polym. Sci.* **2002**, *280*, 282−289.
(3) Boal, A. K.; Ilhan, F.; DeRouchey, J. E.; Thurn-Albrecht, T.; Russell, T. P.; Rotello, V. M. *Nature* **2000**, *404*, 746−748.
(4) Boal, A. K.; Frankamp, B. L.; Uzun, O.; Tuominen, M. T.; Rotello, V. M. *Chem. Mater.* **2004**, *16*, 3252−3256.
(5) Frankamp, B. L.; Uzun, O.; Ilhan, F.; Boal, A. K.; Rotello, A. M. *J. Am. Chem. Soc*. **2002**, *124*, 892−893.
(6) Mori, H.; Lanzendörfer, M. G.; Müller, A. H. E. *Langmuir* **2004**, *20*, 1934−1944.
(7) Tamaki, R.; Chujo, Y. *Chem. Mater.* **1999**, *11*, 1719−1726.
(8) Cao, Y. W.; Jin, R.; Mirkin, C. A. *J. Am. Chem. Soc*. **2001**, *123*, 7961−7962.
(9) Shenhar, R.; Norsten, T. B.; Rotello, V. M. *Adv. Mater.* **2005**, *17*, 657−669.
(10) Shenhar, R.; Rotello, V. M. *Acc. Chem. Res.* **2003**, *36*, 549−561.
(11) (a) Frankamp, B. L.; Boal, A. K.; Rotello, V. M. *J. Am. Chem. Soc.* **2002**, *124*, 15146−15147. (b) Krasteva, N.; Besnard, I.; Guse, B.; Bauer, R. E.; Müllen, K.; Yasuda, A.; Vossmeyer, T. *Nano. Lett.* **2002**, *2*, 551−555. (c) Vossmeyer, T.; Guse, B.; Besnard, I.; Bauer, R. E.; Müllen, K.; Yasuda, A. *Adv. Mater*. **2002**, *14*, 238−242.
(12) Galow, T. H.; Drechsler, U.; Hanson, J. A.; Rotello, V. M. *Chem. Commun*. **2002**, 1076−1077.
(13) Srivastava, S.; Verma, A.; Frankamp, B. L.; Rotello, V. M. *Adv. Mater.* **2005**, *17*, 617−621.
(14) Mori, H.; Müller, A. H. E.; Klee, J. E. *J. Am. Chem. Soc*. **2003**, *125*, 3712−3713.
(15) Zhu, M.-Q.; Wang, L.-Q.; Exarhos, G. J.; Li, A. D. Q. *J. Am. Chem. Soc*. **2004**, *126*, 2656−2657.
(16) (a) Lee, S. C.; Chang, Y.; Yoon, J.-S.; Kim, C.; Kwon, I. C.; Kim, Y.-H.; Jeong, S. Y. *Macromolecules* **1999**, *32*, 1847. (b) Kim, C.; Lee, S. C.; Kang, S. W.; Kwon, I. C.; Kim, Y.-H.; Jeong, S. Y. *Langmuir* **2000**, *16*, 4792. (c) Lee, S. C.; Kim, C.; Kwon, I. C.; Chung, H.; Jeong. S. Y. *J. Controlled Release* **2003**, *89*, 437−446. (d) Liu, S.; Weaver, J. V. M.; Save, M.; Armes, S. P. *Langmuir* **2002**, *18*, 8350−8357. (e) Fukushima, S.; Miyata, K.; Nishiyama, N.; Kanayama, N.; Yamasaki, Y.; Kataoka, K. *J. Am. Chem. Soc*. **2005**, *127*, 2810−2811. (f) Bronich, T. K.; Keifer, P. A.; Shlyakhtenko, L. S.; Kabanov, A. V. *J. Am. Chem. Soc*. **2005**, *127*, 8236−8237. (g) Allen, C.; Han, J.; Yu, Y.; Maysinger, D.; Eisenberg, A. *J. Controlled Release* **2000**, *63*, 275−286.
(17) Holappa, S.; Kantonen, L.; Winnik, F. M.; Tenhu, H. *Macromolecules* **2004**, *37*, 7008−7018.
(18) Haglund, A. O.; Joshi, R.; Himmelstein, K. J. *J. Controlled Release* **1996**, *41*, 229−235.
(19) Kim, C.; Lee, S. C.; Shin, J. H.; Yoon, J.-S.: Kwon, I. C.; Jeong, S. Y. *Macromolecules* **2000**, *33*, 7448.
(20) Harada, A.; Kataoka, K. *Macromolecules* **1998**, *31*, 288.
(21) Wilhelm, M.; Zhao, C.; Wang, Y.; Xu, R.; Winnik, M. A.; Mura, J.; Riess, G.; Croucher, M. D. *Macromolecules* **1991**, *24*, 1033.
(22) Shen, H.; Zhang, H.; Eisenberg, A. *J. Am. Chem. Soc*. **1999**, *121*, 2728−2740.
(23) Shibasaki, Y.; Sanada, H.; Yokoi, M.; Sanda, F.; Endo, T. *Macromolecules* **2000**, *33*, 4316−4320.
(24) Kabanov, A. V.; Nazarova, I. R.; Astafieva, I. V.; Batrakova, E. V.; Alakhov, V. Y.; Yaroslavov, A. A.; Kabanov, V. A. *Macromolecules* **1995**, *28*, 2303.
(25) Nagasaki, Y.; Okada, T.; Scholz, C.; Iijima, M.; Kato, M.; Kataoka, K. *Macromolecules* **1998**, *31*, 1473.
(26) Kwon, G. S.; Naito, M.; Yokoyama, M.; Okano, T.; Sakurai, Y.; Kataoka, K. *Langmuir* **1993**, *9*, 945.
(27) Kwon, I. C.; Bae, Y. H.; Kim, S. W. *Nature* **1991**, *354*, 291.
(28) Kim, C.; Lee, S. C.; Kwon, I. C.; Chung, H.; Jeong S. Y. *Macromolecules* **2002**, *35*, 193−200.
(29) Freichel, O. L.; Lippold, B. C. *Int. J. Pharm.* **2001**, *216*, 165−169.
(30) Sakuma, S.; Hayashi, M.; Akashi, M. *Adv. Drug Delivery Rev*. **2001**, *47*, 21−37.

MA051380H